Proceedings of the ASME 2010 3rd Joint US-European Fluids Engineering Summer Meeting and 8th International Conference on Nanochannels, Microchannels, and Minichannels
FEDSM-ICNMM2010
August 1-5, 2010, Montreal, Canada

FEDSM-ICNMM2010-30675

EFFECT OF BIFURCATION ON PULSE WAVE PROPAGATION IN HUMAN ARTERIES

Yusuke Kawai
Department of Mechanical Engineering,
The University of Tokyo
Hongo 7-3-1, Bunkyo-ku, Tokyo 113-8656, Japan

Shigehiko Kaneko
Department of Mechanical Engineering,
The University of Tokyo
Hongo 7-3-1, Bunkyo-ku, Tokyo 113-8656, Japan

ABSTRACT

In recent years, arteriosclerotic cardiovascular disease becomes a serious problem in the developed countries. The degree of the arteriosclerosis should be examined routinely and invasively, and the measurement of pulse wave is considered as an effective estimation method. Nowadays, pulse wave is widely used in clinical practice as a noninvasive method of examining circulatory kinetics, but the mechanism in the process of the systolic wave generated at heart and propagating to the peripheral artery remains to be elucidated. In this research, to investigate the effect of bifurcation on pulse wave propagation, numerical simulations by a dynamic model of arteries and in vitro experiments were conducted. A one-dimensional model of arteries is coupled by partial differential equations describing mass and momentum conservation with the tube law that relates the local cross-sectional area to the local radial pressure difference. In the case of a bifurcated artery model, the governing equations were solved by introducing the momentum caused by the reactive force at bifurcation into the equation of momentum conservation. The momentum by the reactive force at bifurcation was supposed to be proportional to the momentum flowing into the bifurcation, and the proportionality coefficient was derived from experiments. Then, the proposed one-dimensional model was validated by a comparison to experimental data. In the experimental setup, elastic tubes with different values of Young's modulus were tested to simulate human arteries. From the numerical and experimental results, it turns out that the characteristic waveforms of the pressure and velocity obtained from experiments are also captured by the numerical calculations.

INTRODUCTION

Recently, arteriosclerotic cardiovascular disease becomes a serious problem in developed countries. In such a situation, the measurement of pulse wave is highly concerned as the effective method that will examine the degree of the arteriosclerosis routinely and invasively. Pulse wave is widely used in clinical practice as a noninvasive method of examining circulatory kinetics. For example, methods for diagnosing the degree of the arteriosclerosis from the waveform of the second derivatives of pulse waves have been introduced clinically [1, 2]. Although the application of pulse waves attracted many physicians, the mechanism in the process of the systolic wave generation at heart and propagation to the peripheral artery has not yet been clarified. Therefore, it is important to investigate the mechanism of pulse wave propagation for future clinical use.

To study the mechanism of pulse wave propagation, it is necessary to consider the fluid-structure interaction (FSI) between arterial wall and the flow in artery. On the FSI in human vessels, recently, analyses of flow field by numerical simulation employing three-dimensional (3-D) model of human arteries are reported [3, 4, 5]. In such studies, main concern is the stress acting on the vessel wall and flow regime in the vessel. However, the use of 3-D models is limited to local areas of the arterial system mainly because of their computational cost. Therefore, they are not suitable for analyzing a more global phenomenon observed in the cardiovascular system such as pulse wave propagation. On the other hand, one-dimensional (1-D) model offers a good compromise between accuracy and computational cost, so that it is considered to be better suited for the analysis of pulse wave propagation than 3-D model.

Several efforts have been made in the past to analyze pulse wave propagation in the human cardiovascular system by using 1-D model of arteries. Massys et al. [6] constructed the 1-D model of the whole arterial system, and the numerical results were verified by 1:1 *in vitro* experimental model. In other studies, another type of 1-D model of the whole cardiovascular system is proposed [7, 8, 9]. However, in all the 1-D models proposed so far, the effect of reactive force at bifurcation to pulse wave propagation was not take into account.

In this study, the effect of reactive force at bifurcation on pulse waveform was examined both experimentally and numerically and the comparison between numerical and experimental results was made.

NOMENCLATURE

Symbol

A : cross-sectional area of a tube [m^2]
A_0 : cross-sectional area of a tube at natural state [m^2]
Amp : amplitude of velocity wave [m/s]
c : coefficient of viscous damping [kg/(s m^2)]
E : Young's modulus [MPa]
f_{ref} : reactive force at bifurcation [N]
L : tube perimeter [m]
P : pressure [Pa]
pp : peak-to-peak time interval [s]
Q : flow rate [m^3/s]
t : time [s]
u : flow velocity [m/s]
w : tube thickness [m]
x : axial coordinate along the tube [m]
Δt : peak width [s]
ρ : density [kg/m^3]
τ_{wl} : shear stress at tube wall [Pa]

suffix

a : measurement point A
b : measurement point B
ext : external
in : flowing into the bifurcation
inp : input wave
out : flowing out the bifurcation
ref : reflected wave
I : Case I
II : Case II

EXPERIMENTAL MODEL

From the model experiment, the pressure and flow velocity transient waveforms at two locations along the elastic tubes were obtained. The experimental data are treated as comparative data for the pressure and flow velocity waveforms simulated by means of numerical model.

Experimental setup and procedure

The schematic diagram of the experimental setup used in this study to carry out wave propagaton experiments in flexible vessels is shown in Fig. 1. Water was used as working fluid. The water was controlled at 30 degrees Celsius by a heater, and pumped from the water tank to the upstream reservoir. The reservoir height was controlled to maintain a constant pressure head at the the inlet of the tube. Before the inlet of the elastic tube, a stepping motor was equipped to drive a piston to generate a pulse wave and send into the elastic tube. Then, a pulse wave propagates inside the elastic tube. As an initial pulse wave, half sinusoidal single pulse was adopted and the signal of the initial pulse was generated by a PC. The elastic tube was placed in horizontal position inside a container filled with water to cancel the effect of gravity. The tube is fixed in both sides and can expand freely in the radial direction along its length. On the way the pulse wave propagating to the outlet of the tube, the fluctuations of pressure and flow velocity were measured simultaneously by pressure sensor and hot-wire anemometer. All experiments were conducted under the conditions shown in Table 1, which is set to be similar to the conditions in human body.

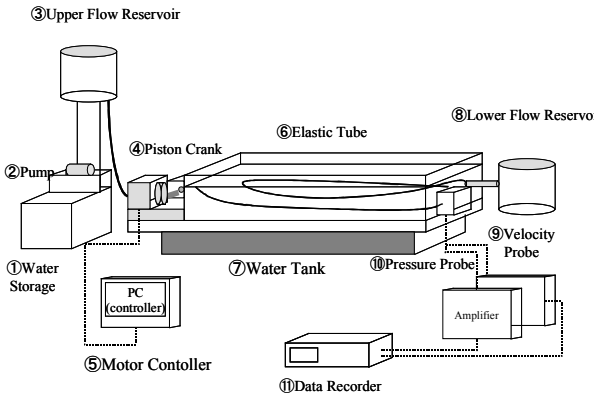

Fig. 1 Schematic of experimental device.

Table 1 Experimental conditions

	Exp. Setup	Human Body
Pulse Period [s]	0.3	0.3～1
Mean Inner Pressure [kPa]	6.8	About 13.3
Pulse Amplitude [kPa]	1.5	About 6.8
Inner Diameter of the tube [mm]	5	2～6
Thickness of the tube [mm]	1	5～10% of the inner diameter
Flow Velocity [m/s]	0.25～0.82	- 0.18～0.92
Young's Modulus (Sim.) [MPa]	4.0, 5.0	0.07～19.8
Young's Modulus (Exp.) [MPa]	4.0, 4.4	0.07～19.8

To investigate the effect of bifurcation on pulse wave propagation, single straight tube and bifurcated tube were used as shown in Fig. 2. In addition, two kinds of material with different Young's modulus were tested to examine the effect of wall elasticity (Table 2).

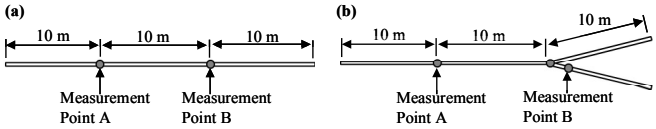

Fig. 2 Shapes of elastic tubes for the experiment : (a) single straight tube, (b) bifurcated tube.

Table 2 Young's modulus of the elastic tubes

	Young's modulus [Mpa]
Silicon tube	4.0
Eco tube	4.4

NUMERICAL MODEL

In this study, the flow in an artery was described by a one-dimensional model that has been proved suitable for describing wave propagation phenomena in arteries [3, 6, 7].

Governing equations

One-dimensional governing equations for blood flow in the artery can be obtained by integrating the mass conservation equation and the momentum equation over a cross-section of the artery.

$$\frac{\partial A}{\partial t}+\frac{\partial (uA)}{\partial x}=0 \tag{1}$$

$$\rho\left(\frac{\partial u}{\partial t}+u\frac{\partial u}{\partial x}\right)=-\frac{\partial P}{\partial x}-\tau_{wT}\frac{L}{A} \tag{2}$$

The system of governing equations can be completed with the pressure-area relationship. It assumes a thin, homogeneous and elastic arterial wall and it takes the form as follows [10],

$$P-P_{ext}-c\frac{\partial A}{\partial t}-\Phi(A)=0 \tag{3}$$

Here, $\Phi(A)$ is

$$\Phi(A)=wE\sqrt{\frac{\pi}{A}}\left(1-\sqrt{\frac{A_0}{A}}\right) \tag{4}$$

Treatment of bifurcations

For the case in which the elastic tube has a bifurcation, the following equation was used as a substitute for Eq. (2).

$$\rho\left(\frac{\partial u}{\partial t}+u\frac{\partial u}{\partial x}\right)=-\frac{\partial P}{\partial x}-\tau_{wT}\frac{L}{A}-f_{ref} \tag{5}$$

Here, f_{ref} represents the reactive force acting to the fluid at the bifurcation. Assuming that f_{ref} is proportional to the momentum flowing into the bifurcation, the following equation can be obtained

$$f_{ref}=k\rho Q_{in}u_{in}=k\rho A u_{in}^2 \tag{6}$$

where, k denotes a proportionality coefficient obtained by a set of experimental results mentioned below. Flow conditions at the bifurcation were described by mass conservation and total pressure continuity as follows,

$$Au_{in}=2Au_{out} \tag{7}$$

$$P_{in}+\frac{1}{2}\rho u_{in}^2+f_{ref}=P_{out}+\frac{1}{2}\rho u_{out}^2 \tag{8}$$

Fig. 3 shows the schematic diagram of the experimental setup used to identify the coefficient k. In this experiment, velocity and pressure before and after the bifurcation were measured by the pressure sensor and hot-wire anemometer. The experimental conditions for this experiment are listed in Table 3. Then, k was derived by means of Eq. (6) ~ (8) and experimental results and finally its value was identified to be 0.375 as can be found in Fig. 4.

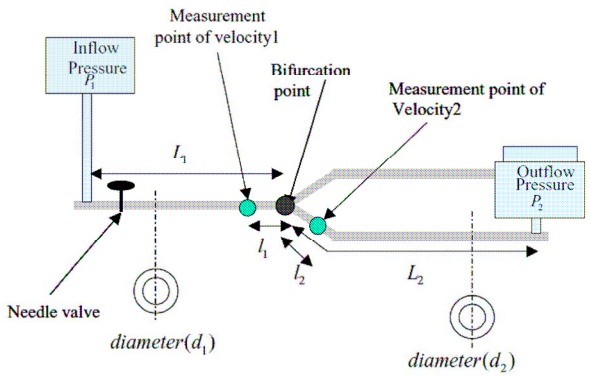

Fig. 3 Schematic of experimental setup for the identification of the proportionality coefficient *k*.

Table 3 Experimental conditions in the experiments for the identification of the proportionality coefficient *k*.

Parameters	value
Inflow pressure P_1 [Pa]	13334
Outflow pressure P_2 [Pa]	3400
Inner diameter d_1 [mm]	5.0
Inner diameter d_2 [mm]	7.0
Length of the upstream tube L_1 [m]	1.0
Length of the downstream tube L_2 [m]	0.5
Distance between bifurcation point and measuring point l_1 [m]	0.1
Distance between bifurcation point and measuring point l_2 [m]	0.1

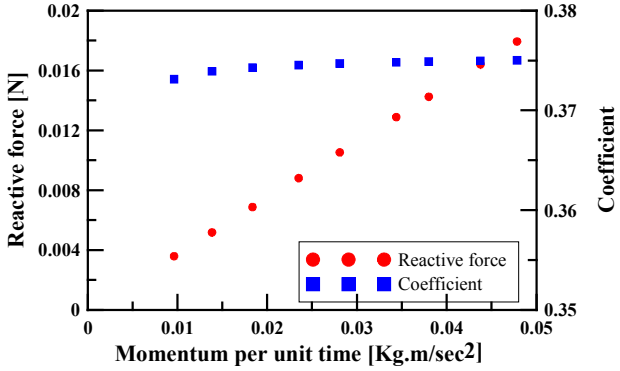

Fig. 4 Proportionality coefficient *k* and reactive force f_{ref} in the silicon tube.

RESULTS

The case of straight tube

First, experiments and numerical simulations of pulse wave propagation with the straight tube were carried out. The results are shown in Fig 5, and Fig. 6. In both experimental and numerical results, input wave, reflected wave, and back-flow wave were observed as characteristic waves of pressure and velocity. Here, the input wave represents a wave propagation of initial pulse and the reflected wave corresponds to the wave in which input wave was reflected at the downstream tank. In addition, the back flow wave represents the wave observed a few seconds after the input wave, and it propagates against the direction of the streaming flow. In the following, the details of the result are considered.

Experimental results using a silicon tube are shown in Fig.5(a), (b). As can be found in this figure, at measurement point A, the input wave, the back-flow wave, and the reflected wave were observed at 1.0, 1.3, and 2.3 seconds after the measurement start. Similarly, at measurement point B, the input wave and the reflected wave were observed at 1.3 and 2.0 seconds after the measurement start.

Numerical results in the case that Young's modulus of the elastic tube is 4 MPa are shown in Fig.5(c), (d). In the same way as the experimental results, at measurement point A, the input wave, the back-flow wave, and the reflected wave were observed at 0.7, 0.8, and 2.7 seconds after the measurement start. Similarly, at measurement point B, the input wave, the back-flow wave, and the reflected wave were observed at 0.7, 0.8, and 1.8 seconds after the measurement start.

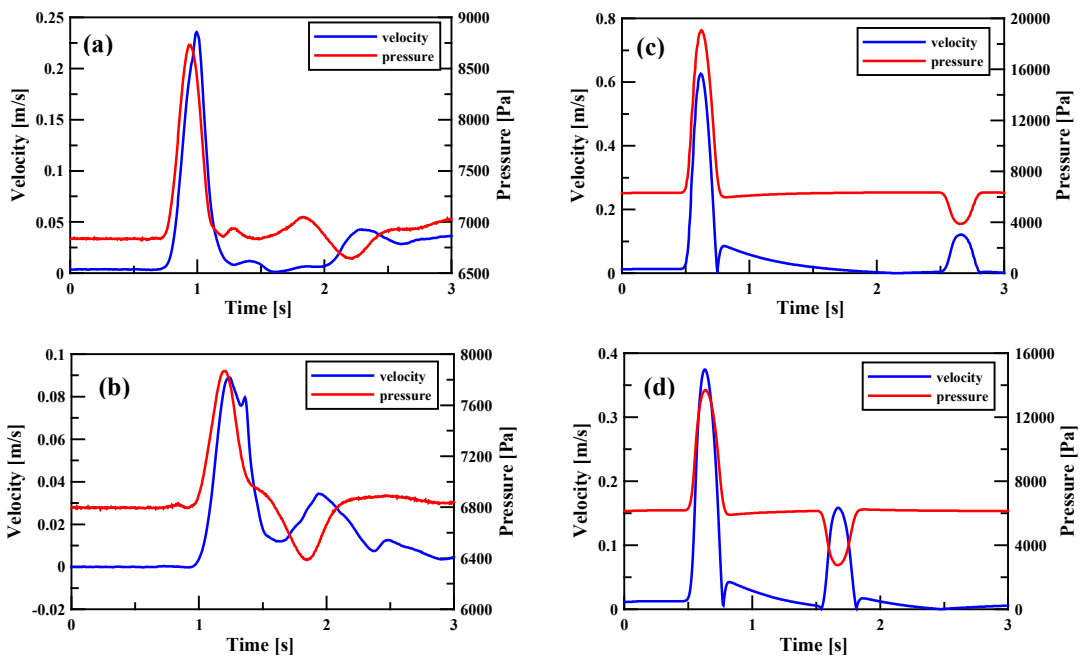

Fig. 5 Velocity and Pressure wave in straight silicon-tube obtained by experiments (left) : (a) measurement point A, (b) measurement point B. Velocity and Pressure wave in the straight tube with 4 MPa of Young's modulus obtained by calculations (right) : (c) measurement point A, (d) measurement point B.

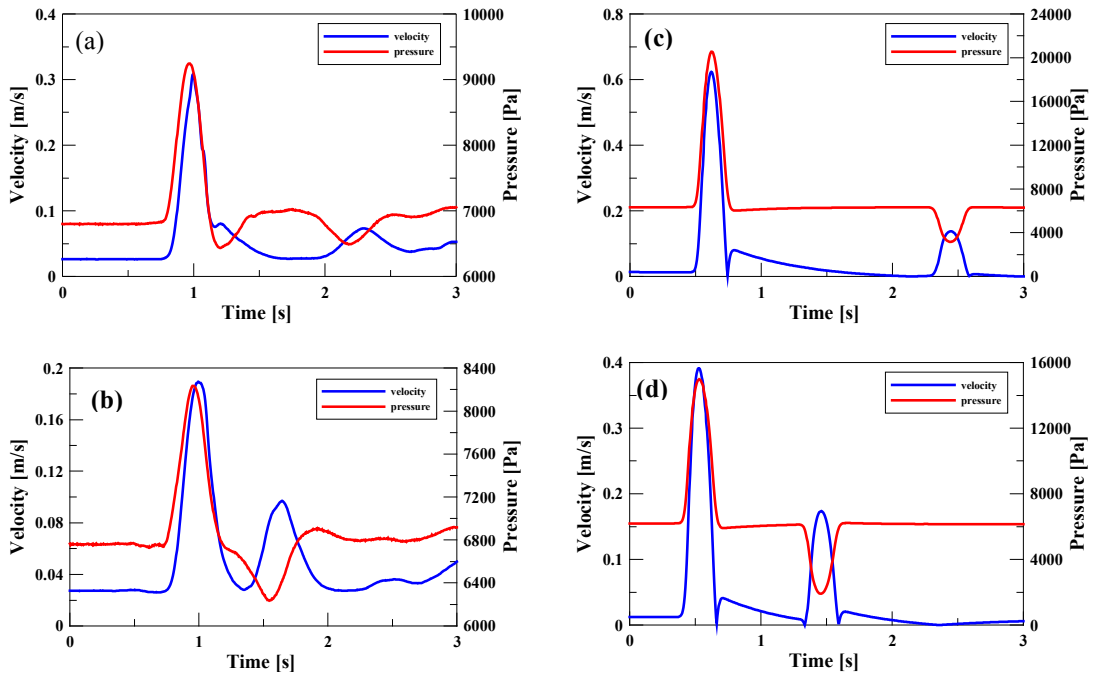

Fig. 6 Velocity and Pressure wave in straight eco-tube obtained by experiments (left) : (a) measurement point A, (b) measurement point B. Velocity and Pressure wave in the straight tube with 5 MPa of Young's modulus obtained by calculations (right) : (c) measurement point A, (d) measurement point B.

Additionally, experimental and numerical results in the tubes of different Young's modulus are shown in Fig. 6. Comparing the waveforms in Fig.5 with that in Fig.6, the following things are found. First, pulse wave velocity becomes faster with larger values of Young's modulus. Second, with the increase of Young's modulus, the damping effect becomes smaller.

From the above observations, it turns out that the characteristic waveforms of the pressure and velocity obtained from experiments are also captured by the numerical calculations.

The case of bifurcated tube

Experiments and numerical simulations of pulse wave propagation with bifurcated tube were conducted. The results are shown in Fig. 7,and Fig. 8. In the case of bifurcated tube, the reflected wave at the bifurcation was observed besides the characteristic waves in the case of straight tube.

In order to explain the characteristics of waves observed from experiments, velocity and pressure wave obtained by pulse wave experiments in the bifurcated tube are shown in Fig. 7(a), (b). At measurement point A, the input wave, the back-flow wave, the reflected wave at the bifurcation and the reflected wave at the downstream tank were observed at 1.0, 1.3, 1.8 and 2.2 seconds after the measurement start. Meanwhile, at measurement point B, the input wave and the reflected wave were observed at 1.0 and 1.6 seconds after the measurement start.

Numerical simulations were examined in the same way as the case of the straight tube. Fig.7(c), (d) show the numerical results in the case that Young's modulus of the elastic tube is 4 MPa. At measurement point A, the input wave, the back-flow wave, the reflected wave at the bifurcation and the reflected wave at the downstream tank were observed at 0.7, 0.8, 1.8 and 2.7 seconds after the measurement start. At measurement point B, the input wave, the back-flow wave, and the reflected wave were observed at 0.7, 0.8, and 1.3 seconds after the measurement start.

As in the case of straight tube, one can find that the characteristic waveforms of the pressure and velocity obtained from experiments are also captured by the numerical calculations with the case of bifurcated tube, and according to the results shown in Fig. 8, the effect of Young's modulus is found also in this case.

Comparison between experiments and simulations

In the following, the results of experiments and numerical simulations were quantitatively evaluated. Regarding the charastaristic wave mentioned above, that is input wave and reflected wave, comparisons between experimental and numerical results were carried out. As evaluation indices, amplitude of the waves, peak width, and peak-to-peak time interval were used for the two case shown in Table 4. Both in the case I and II, comparisons of velocity wave obtained by numerical simulations with that obtained by experiments were conducted. For the case I, amplitude of input wave and reflected wave at the downstream tank, peak width of those waves, and

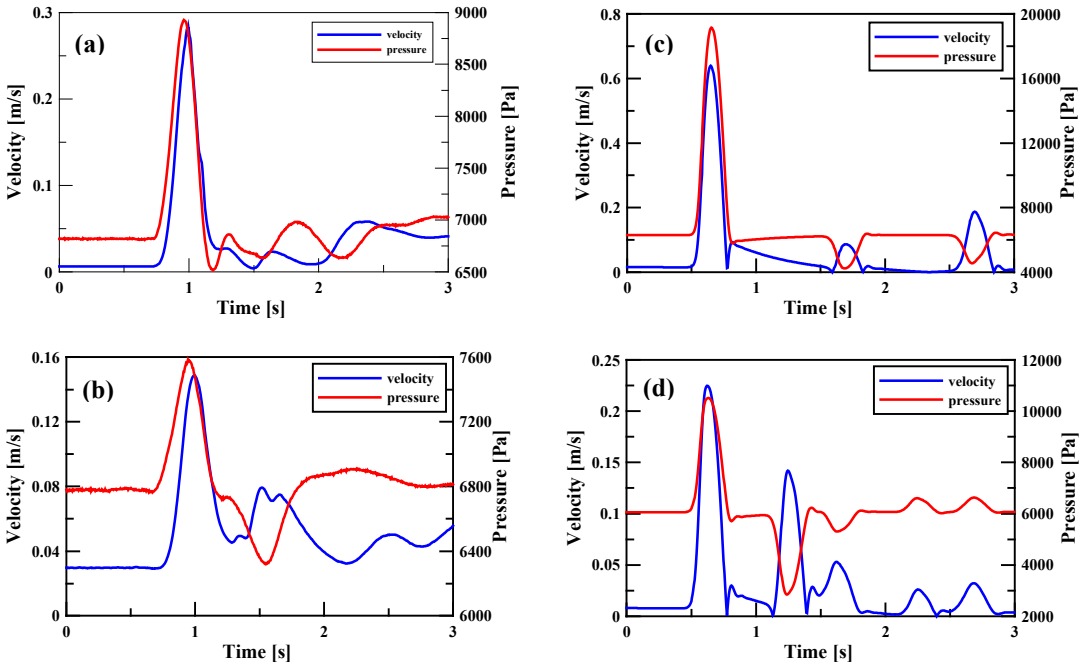

Fig. 7 Velocity and Pressure wave in bifurcated silicon-tube obtained by experiments (left) : (a) measurement point A, (b) measurement point B. Velocity and Pressure wave in the bifurcated tube with 4 MPa of Young's modulus obtained by experiments (right) : (c) measurement point A, (d) measurement point B.

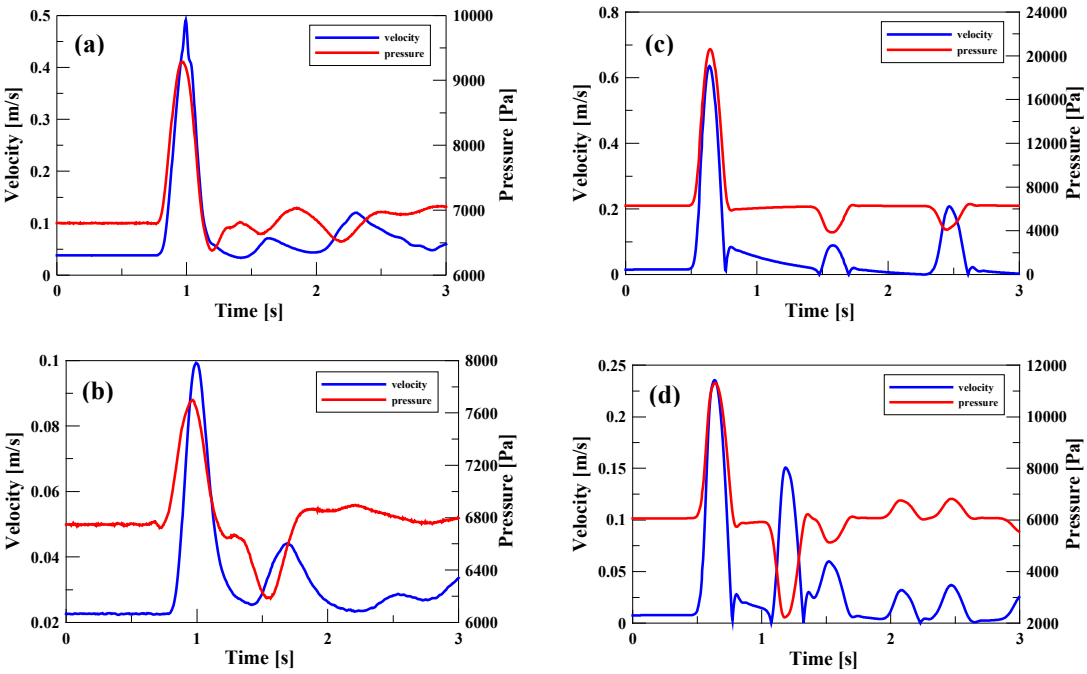

Fig. 8 Velocity and Pressure wave in bifurcated eco-tube obtained by experiments (left) : (a) measurement point A, (b) measurement point B. Velocity and Pressure wave in the bifurcated tube with 5 MPa of Young's modulus obtained by calculations (right) : (c) measurement point A, (d) measurement point B.

peak-to-peak time interval from input wave to reflected wave at the downstream tank were used as indices, $Amp_{I,inp}$, $Amp_{I,ref}$, $\Delta t_{I,inp}$, $\Delta t_{I,ref}$, and pp_I, respectively. For the case II, amplitude of input wave and reflected wave at the bifurcation, peak width of those waves, and peak-to-peak time interval from input wave to reflected wave at bifurcated wave were used as indices, $Amp_{II,inp}$, $Amp_{II,ref}$, $\Delta t_{II,inp}$, $\Delta t_{II,ref}$, and pp_{II}, respectively. The values of those index in each case and ratio of simulated value to experimetal value are shown in Table 5 and Table 6.

According to Table 5 and Table 6, one can see that amplitude of the waves in the case of simulations is larger than that of experiments, but the other indices in numerical results show accordance to some extent with experiments, comparing to amplitude. It could be thought that amplitude of the waves obtained by simulation became large for the reason that some damping effects, such as loss at the bending part, were not taken into consideration in the numerical model of the flow in tube.

Table 4 The two cases under study for the comparison of simulations with experiments.

	shape of tube	measurement point	Young's modulus
Case I	straight	point A	4 MPa
Case II	bifurcated	point A	4 MPa

Table 5 Comparison between experiment and simulation for the case I

	$Amp_{I,inp}$ [m/s]	$\Delta t_{I,inp}$ [s]	$Amp_{I,ref}$ [m/s]	$\Delta t_{I,ref}$ [s]	pp_I [s]
Experiment	0.231	0.570	0.0361	0.625	1.28
Simulation	0.609	0.265	0.116	0.315	2.01
Ratio	2.63	0.464	3.21	0.504	1.57

Table 6 Comparison between experiment and simulation for the case II

	$Amp_{II,inp}$ [m/s]	$\Delta t_{II,inp}$ [s]	$Amp_{II,ref}$ [m/s]	$\Delta t_{II,ref}$ [s]	pp_{II} [s]
Experiment	0.275	0.495	0.0191	0.435	0.74
Simulation	0.622	0.275	0.0860	0.240	1.09
Ratio	2.26	0.555	4.50	0.551	1.47

CONCLUSIONS

In this study, *in vitro* experiments simulating the artery system and the numerical simulations by 1-D model of the artery specially focused on the effect of bifurcation were carried out. As a conclusion, following results are obtained.

It was attempted to consider the effect of bifurcation on pulse wave propagation by introducing the idea of reactive force acting at the bifurcation into the momentum equation in the flow. As a result, proposed 1-D model can capture the characteristic waveforms of pulse wave, which obtained by *in vitro* experiments simulating human arteries. However, to propose more reliable dynamic model in quantitative sense, other factors currently not included should be considered.

In future works, using the knowledge obtained from the present study, investigation on pulse wave propagation in the entire artery system of a human body will be examined.

REFERENCE

[1] Hashimoto, J., Watabe, D., Kimura, A., Takahashi, H., Ohkubo, T., Totsune, K. and Imai, Y., 2005, "Determinants of the Second Derivative of the Finger Photoplethysmogram and Brachial–Ankle Pulse-Wave Velocity: The Ohasama Study", American Journal of Hypertension, **18**, pp. 477-485.

[2] Oh-i, T., Okuda, T., Shimazu, H. and Watanabe, A., 2002, "An experimental study of vascular dynamics by an acceleration plethysmogram using artificial circulation devices", Life Sciences, **71**, pp. 1655–1666.

[3] Formaggia, L., Gerbeau, J. F., Nobile, F. and Quarteroni, A., 2001, "On the coupling of 3D and 1D Navier-Stokes equations for flow problems in compliant vessels", Computer methods in applied mechanics and engineering, **191**, pp. 561-582.

[4] Marzo, A., Luo, X. Y. and Bertram, C. D., 2005, "Three-dimensional collapse and steady flow in thick-walled flexible tubes", Journal of Fluids and Structures, **20**, pp. 817-835.

[5] Bathe, M. and Kamm, R. D., 1999, "A Fluid-Structure Interaction Finite Element Analysis of Pulsatile Blood Flow Through a Compliant Stenotic Artery", ASME Journal of Biomechanical Engineering, **121**, pp. 361-369.

[6] Matthys, K. S., Alastruey, J., Peiro, J., Khir, A. W., Segers, P., Verdonck, P. R., Parker, K. H. and Sherwin, S. J., 2007, "Pulse wave propagation in a model human arterial network: Assessment of 1-D numerical simulations against invitro measurements", Journal of Biomechanics, **40**, pp. 3476-3486.

[7] Sherwin, S. J., Franke, V., Peiro, J. and Parker, K., 2003, "One-dimensional modelling of a vascular network in space-time variables", Journal of Engineering Mathematics, **47**, pp. 217-250.

[8] Stergiopulos, N., Young, D. F. and Rogge, T. R., 1992, "Computer simulation of arterial flow with applications to arterial and aortic stenosis", Journal of Biomechanics, **25**, pp. 1477-1488.

[9] Liang, F., Takagi, S. and Himeno, R., 2009. "Multi-scale modeling of the human cardiovascular system with applications to aortic valvular and arterial stenoses", Medical & Biological Engineering & Computing, **47**, pp. 743-755.

[10] Matsuzaki, Y. and Matsumoto, T., 1989, "Flow in a two-dimensional collapsible channel with rigid inlet and outlet", ASME Journal of Biomechanical Engineering, **111**, pp. 180-18.